CONDENSED-PHASE LASER IONIZATION TIME-OF-FLIGHT MASS SPECTROMETRY OF HIGHLY ENERGETIC NITROAROMATIC COMPOUNDS

Tomás Delgado, J.F. Alcántara, José M. Vadillo, J. Javier Laserna

Department of Analytical Chemistry, University of Málaga, 29071 Málaga, Spain

RATIONALE

Analysis of explosive compounds represents an interesting field of work due to their high internal energy and obvious social relevance. Direct laser ionization allows their analysis without sampling or preparation procedures. We have performed studies on nitro-aromatic compounds to understand their mass spectra when directly ionized as condensed phase, at a difference of the gas-phase studies commonly conducted. The results have resulted adequate for fast screening in forensic applications.

METHODS

Direct condensed-phase laser ionization time-of-flight mass spectrometry of high energy density materials has been performed using a 5 ns width quadrupled Nd:YAG laser. No matrix assistance was used. Fine control of the laser energy has allowed the study of the fragmentation processes from values close to the ionization threshold to ones where atomic-only mass spectra were recorded.

RESULTS.

The influence of the variation of extraction conditions on the recorded mass spectra has been investigated. For low extraction width pulse values, ions with low mass-charge ratio were observed mainly, whereas at higher width values, higher molecular fragments are also visualized while the total ion current is maintained. Therefore, the mass spectra can be modulated under certain conditions to obtain mass spectra containing molecular or atomic information. The onset of ion generation for the different fragments was also studied, yielding to studies that can help to understand the processes involved in the fragmentation pathways of the molecule and in the dissociation mechanisms. For forensic applications, two sampling procedures where used that allow

the prospective use of LIMS as a screening technique for nitro aromatic-based highly energetic explosives.

CONCLUSIONS

Direct analysis of explosive compounds has been performed by laser ionization. A large dependence of the resultant spectra has been observed when the laser energy changes, what may be useful for studies of fragmentation pathways. For forensic applications, two sampling procedures may allow a prospective use as a screening technique.

Keywords: Laser ionization; High energy density materials, Explosives

INTRODUCTION

The analysis of energetic compounds has been always an important task due to the interesting chemistry associated to their high internal energy.[1] Thermal decomposition chemistry is fundamentally important in the explosives field, and the determination of the kinetics and mechanism of the thermal decomposition remains a fundamental aspect of their characterization. Laser-based mass spectrometry has proved itself to be rather versatile in the characterization of these families of compounds.[2] Moreover, the use of mass spectrometry in studies of the products of decomposition and detonation of explosives has been of considerable importance as it helped to understand the chemical fragmentation pathways which lead to the dissociation of the parent molecules.[3,4] Additionally, explosives detection represents a complex field where analytical chemistry has to face the forensic problem of analyzing the fragments of compound once the explosion has taken place.[5] Conventional analyses is based on well-defined sampling procedures and further analysis in the laboratory mainly consisting on mass spectrometry in combination to gas chromatography and tandem mass spectrometry for confirmation.[6] However, the availability of direct analysis techniques for previous screening performed directly on the condensed-phase samples provide several benefits as reduction in the sample manipulation, and limiting in the sources of contamination. In the situation of a possible positive detection, specific confirmatory techniques may be directly applied, redounding in a significant save in resources, samples and time.

Laser ionization and mass spectrometry (LIMS) represents a happy marriage for condensed-phase analysis. In the field of elemental (atomic) or molecular analysis of solid samples, different works have proved the extraordinary capabilities of LIMS that combines speed, sensitivity, good lateral resolution and in-depth capabilities in the sub-micrometric regime.[7,8]. Despite its apparent simplicity, the transfer of the atoms or molecules of the sample in condensed phase into ions in gas-phase under vacuum conditions, it is a dauntingly complex phenomenon that suffer from interdisciplinary niche status (neither mainstream chemistry nor physics) and demands to be fully understood by diverse approaches different that the simple generation of mass spectra under a variety of experimental conditions.[9,10].

Laser ionization mass spectrometry has been used in the past to study energetic materials in gas phase by means of nanosecond laser pulses. This method allows the rapid screening of many samples without the need of complicated preparation techniques. In the particular case of nitro-related compounds, their fast dissociative states in the neutral excited state[11] have been always being considered an inherent difficulty as the parent ion and molecular fragments were not visible in the recorded mass spectra. In this sense, femtosecond excitation has been always proposed as the only alternative to overcome the commented problem in gas-phase. However, condensed-phase ionization may involve a larger number of processes than those involved in gas-phase photo-ionization that changes completely the panorama of the ionization. The recording of full range mass spectra at increased controlled fluences and temporal extraction conditions allows the establishment of the ionization threshold for the different desorbed ions of the molecule, the generation of atomic/molecular mass spectrum and a deeper understanding about the energetic channels taking place and possible fragmentation pathways. Under this picture, a detailed study of the condensed-phase analysis of explosive compounds via nanosecond laser ionization was performed with the purpose on understanding the effect of different experimental parameters on the resultant mass spectra in the aim of finding the best excitation conditions for direct surface mass spectrometry of explosive compounds.

EXPERIMENTAL

Details on the instrument can be found elsewhere.[12] Figure 1 sketches the most relevant elements of the instrument. Briefly, a pulsed Nd:YAG (5ns, 266nm) laser is used as ionization source. The laser energy was controlled in the interval between 0.3 and 8 mJ using a variable attenuator that allows continuous variation of the energy per pulse without modifications in the beam spatial profile. Care was taken to avoid excess of energy that could induce plasma shielding.[13] The target is placed inside an ionization chamber connected to the flight-tube. Laser was focused on the sample at normal incidence, and the generated ions are orthogonally extracted into the flight-tube (Figure 2). The lens-to-sample distance is slightly shorter (17 mm) than the focal length of the focussing lens (20 mm) in order to avoid tight focusing that may induce fragmentation and explosive ablation conditions. The distance from the laser incidence point and the extraction electrode is controlled by a micrometric stage. Typically is kept at 1 cm. The detector output fed a 500-MHz Digital Phosphor Oscilloscope, controlled externally by home-designed software. Averages of 200 mass spectra (associated to 200 laser events at a frequency rate of 10 Hz) were acquired for every data point. Care was taken to record all the spectra under identical laser excitation and focusing conditions.

SAMPLES

Samples were grinded in an agate mortar to reduce the grain size and facilitate subsequent pelleting. Pellets of 2 mm thickness and 10 mm in diameter were done by weighting 0.4 g of the different compounds and pressing it at 2 atm for 15 minutes. This procedure allows risk-free and safe handling of the compounds. For direct sampling for surfaces, conductive tape consisting of a 50 µm thick aluminum foil with a 50 µm thick electrically conductive acrylic based pressure sensitive adhesive backing was used, following a procedure previously described.[14]

RESULTS AND DISCUSSION

It has been commented in the introduction of this work that most of the bibliography related to the studies of explosive compounds by laser mass spectrometry have been performed by gas-phase photo-ionization by direct flow using a leak valve or by the use of Knudsen cells in the ionization region. Our approach implies the direct analysis of the explosives in condensed phase where a limited number of references have been found.[15] In condensed-phase ionization, the laser impinges the sample generating a significant pool of neutrals and a limited number of ions that can be directly detected. However, the possibility of direct photo-ionization of the desorbed neutrals by non-resonant absorption from their ground state in gas-phase cannot be ruled out. To check the extension of this process in our experiment, the laser beam was redirected so that it passed close to the surface of the sample, a pellet of 2,6 DNT. This compound exhibited a high vapor pressure that impaired the operation of the ionization chamber at vacuum better than 2,5 x 10^{-4} mbar. Thus, it is expected that the UV photons find a significant population of 2,6 DNT in gas phase in the vicinity of the sample surface available for direct absorption. However, no evidence of ion formation was found even at the maximum fluence achievable by our experimental setup (12 J/cm^2). Thus, all the ions generated after direct laser irradiation of the sample are exclusively attributed to those formed as a consequence of the laser-matter interaction.

The lack of ions directly generated by gas-phase photo absorption does not imply the absence of these photo-mechanisms in the solid combined with thermal-induced processes. Considering the fluences used in our experiment, two-photon absorption process would be possible. In the case of 2,6-DNT, although its ionization potential (9.8 eV) can not be reached by absorption of two 266 nm photons (9.30 eV), it must be reminded that the accuracy of calculations is always open to question, and that the free molecule may not be the chemical form to be ionized. Under these premises, a combined photo/thermal mechanism can be considered for ion generation in our sample where the thermal energy of the expanding plume may supply the energy to make up the difference between the ionization potential and the two-photon absorption. Additionally, at higher laser fluences, electron generation in the focal volume may induce electron-ionization like mechanisms with extensive fragmentation yielding atomic-only information in the mass spectrum. This effect is more prominent as the laser wavelength is larger. Comparative experiments performed at laser energies 1.5 times higher than the threshold one (see above discussion) at 1064, 532 and 266 nm, yielded that the UV output was the only one providing useful results. Thus, using 1064 and 532 photons, the spectra was dominated by broad signals at m/z 1, 12, 14 and 16, corresponding to $^{1}H^{+}$,$^{12}C^{+}$, $^{14}N^{+}$ and $^{16}O^{+}$, in accordance with previous works.[16]. Additionally, a fragment at m/z = 30 ($^{30}NO^{+}$) was also observed at low intensity. At 266 nm, intense signals from $^{30}NO^{+}$ and $^{12}C^{+}$ were recorded, as well as a group of low-mass ions corresponding to aromatic compounds (C_nH_m) and molecule fragmentation.

The amount of energy reaching the sample is a key parameter in direct laser desorption/ionization. Differences of few microjoules may change drastically the information contained in the mass spectra. The laser energy per pulse can be easily controlled in our set-up what allows a precise calculation of the minimum laser energy required to record a measurable signal[12] and the evolution of the ion signal with laser energy. The onset of ion generation (ionization threshold) was determined by increasing the energy per pulse reaching the sample while monitoring full-range mass spectra. Due to the use of an optical attenuator, the spatial profile of the laser beam was not modified regardless the energy output. The experiment was performed starting from energy per pulse providing no ion signal in our TOFMS system (lower than 0.2 mJ/pulse for all the studied compounds) and was raised progressively to a maximum of 7 mJ/pulse. This maximum limit was due to excessive plasma formation in the ionization chamber that did induce electrical contact between isolated electrodes. For each new energy setting, the entrance of the laser beam was blocked, and 200 consecutive shots were monitored to determine the average energy per pulse and the relative standard deviation (RSD) of the data. Typically, RSD values lower than 1% was obtained. The laser diameter at the sample surface was determined by irradiating a Cu foil and measuring the affected area with an optical microscope. Due to the low energy per pulse, overestimation of the laser spot due to heating effects was discharged. The resultant beam diameter was 280 μm, corresponding to an area of 6.15 x10^{-4} cm^2.

Figure 3 shows the changes in the recorded mass spectrum for 2,6-DNT when the energy per pulse is raised in the vicinity of the ionization threshold. It is expected that low fluence leads only to desorptive ion emission from the sample surface, while ions deeper in the material are not released. Only when ablative phase explosion becomes widespread can a larger fraction of the available ions reach the gas phase. Early ion signal (corresponding to the surface desorption of $^{23}Na^+$) demands a minimum energy per pulse of 0.30 mJ (0.49 J/cm^2). From 0.35 mJ/pulse (0.57 J/cm^2), apart from the ubiquitous $^{23}Na^+$ signal, incipient ion signals corresponding to molecular fragments as $^{30}NO^+$, and signals at m/z= 39, 63, 77 corresponding to $C_nH_m^+$ hydrocarbon radicals are observed.[15-17] The low-mass ions series for aromatic compounds are not restricted to specific m/z values, but they are nonetheless consistent enough to be useful for identification of aromatic compounds. The origin of these fragments can be both fragments from the 2,6 DNT or any aromatic residue in the compound. Increasing the energy to 0.40 mJ/pulse (0.65 J/cm^2), a well-resolved mass spectrum is observable with information in the high mass range. As in related references,[2,4,17-19] our spectra does not show signals associated to $^{46}NO_2$. This fact it is due to the short lifetime of the intermediate states involved in the generation of NO_2^+(a few hundred femtoseconds), that leads a to rapid dissociation to generate the most stable NO^+ion.[19]

Additional energy per pulse is required to generate the molecular peak, as it may be observed in Figure 4 for the different mass spectrum recorded at selected energies per pulse covering values up to 7 mJ/pulse. It is quite obvious the richer mass information obtained with increasing the energy per pulse. However, a higher fragmentation, visible as contributions at m/z < 20, it is also occurring. Due to the balance between sensitivity, full mass-range information and fragmentation, a value of 1.3 mJ/pulse was taken for further experiments.

Figure 5 shows the threshold for specific evolution of specific m/z with increasing energy per pulse for $^{12}C^+$, $^{30}NO^+$, $^{63}C_5H_5^+$ and $^{148}(M\text{-}2OH)^+$. It is quite clear the presence of $^{30}NO^+$, $^{63}C_5H_3^+$

and ^{148}(M-2OH)$^+$ at low energies per pulse, experimenting the four peaks a sudden intensity increase at about 0.75 mJ/pulse. From this point, different behaviour is observed. The ^{148}(M-2OH)$^+$ fragment exhibits a maximum around 1.3 mJ/pulse, decreasing quite sharply its intensity, reaching zero at about 3 mJ/pulse. The same behaviour was found for the ^{165}(M-OH)$^+$ fragment. The $^{30}NO^+$ signal increases up to 2.20 mJ/pulse, dropping afterwards. It is interesting to note in Figure 4 that all the plots modify their trends at about 1 mJ/pulse. Depending on the monitored ion, this cut-off value corresponds to a change in the slope (as in m/z = 63), the onset of ion generation (m/z = 12) or the starting of the ion extinction (m/z = 163).The fact that the ^{12}C signal (evidencing full fragmentation of chain fragments) starts at this cut-off value supports the idea of a change in the ablation mechanism corresponding to Coulomb explosion.

The orthogonal extraction geometry used in our experiment allows a decupling of the initial kinetic energy of the ions due to their escape velocities from the solid and the one provided by the extracting field. Even under near threshold conditions, the kinetic energy and spread of the ions is large once Coulomb explosion occurs. Thus, the pulse amplitude, length and delay with respect to the laser incidence are important parameters to account in orthogonal extraction that can modify quite dramatically the signal intensity of the detected ions. In our experiments, it was observed that the ion yield decreased significantly as soon as delays larger than 100 ns were introduced. No attempts were done to modify the geometry of the extraction lens with respect to the sample. Thus, the zero delay condition was kept for all the experiments. The amplitude of the extraction voltage was very sensitive up to a given voltage where the signal reached a plateau that was selected as optimum extraction amplitude. The most significant effect was observed in the pulse width. Figure 6 shows the full mass spectrum at increasing pulse widths from 400 ns to 2000 ns. For values lower than 400 ns the signal was quite unstable probably due to instabilities on the electronics of the high power switch at these low values. At 400 ns, the spectrum reveals exclusively atomic information, while progressive richer information at the high mass range is obtained as the extraction width is larger. No changes were observed when the width was increases over the 2000 ns value.

The full explanation to this experimental fact still remains unclear although several facts can be taking into account. First, the surface of the sample pellet is aligned with the geometrical centre of the extracting electrode that has an internal diameter of 1.5 cm. Overestimating the escape velocities of the formed ions in 1 μm/ns based on MALDI ions measurements[20] and considering no momentum loss during the expansion, we can assert that the ions will be under the effect of the orthogonal extractive grid during 7.5 ms after the hitting of the laser with the sample. So, the ions will be efficiently deflected to the field-free region of the analyzer with the extractive pulse widths commented. A second factor to consider is the different distribution of species along the expanding plasma. The high temperatures and electron density favours the formation of atomic species close to the surface. As long as the expansion plume takes place, the secondary mechanisms in the plume gain relevance. The question to be solved in future studies is the understanding of the extension of the gas-phase processes on the final spectra and how the final mass spectrum is representative of the molecules and particles in the condensed phase. Regardless this matching, the experimental results clearly open the possibility to obtain modulated atomic/molecular spectra.

Figure 7 shows a comparison of the spectra taken at 2000 ns with the 2,6 DNT electron impact spectra from the NIST data base. As shown, the matching in the information is rather satisfactory. The direct link between the chemistry in the gas phase and the reactions taking place in the condensed phase is complex. As commented, the final mass spectrum is a convolution of the early chemistry at the time scale of the laser-mater interaction and a variety of secondary reactions that further degrade the parent molecule. The laser-driven ignition process and the time scale where our measurements is taking place, are a chance for secondary mechanisms to occurs that will enrich the final spectrum with additional features closely related to those occurring under detonation conditions. In this sense, it is our believe that direct ionization on condensed phase coupled to time-of-flight mass spectrometry represents a remarkable tool in the sound understanding of the chemistry of high energetic materials.

It seems that under lab-frame conditions, LIMS may be seen as a fast mass spec based tool for screening purposes prior to a detailed confirmatory analysis. However, our results are based on pressed pellets, a situation unrealistic under forensic analysis conditions, that implies working with surface traces of the sample, and where special sampling conditions are required. Thus, two different approaches have used to the analysis of TNT that could be potentially valid for forensic analysis. In the first one, the sample is collected from the surface in powdered form[14] by using conductive double sided adhesive Al tape, while in the second, the sample recovered from a given surface is dissolved in acetone, spiked (50 μL) on the surface of an untreated aluminium disk and let dried before analysis. Figure 8 shows a single-shot LIMS spectrum of TNT that has been analyzed following both methods. Figure 8a (top) and 8b (bottom) show the analysis using the Al-tape and dried-drop procedures, respectively. As observed, in the first method, although the $^{30}NO^+$ presence clearly may help to trigger a security protocol due to the presence of nitro-compounds, little molecular information is found. When the dried-drop method was used, it was clearly observable the $^{210}[TNT\text{-}OH]^+$ fragment, as well as the $^{27}Al^+$ from the substrate. Larger energy values led to the absence of any signal from the explosive residue. Modifications in the extraction conditions did not produced any effect but the loss of overall intensity.

CONCLUSIONS

Nanosecond time-of-flight mass spectra of 2,6 DNT have been acquired using the 5 ns fourth-harmonic output from a Nd-YAG laser for one-step desorption/ionization. The work has demonstrated the ability of the technique to generate analyte molecular and structure-specific ions of the nitrocompound (as compared with the electron impact data). The onset of the ion generation for different fragments takes place at the same laser energy (~ 0.35 mJ, 0.53 J/cm^2). The opening of the aromatic ring seems to occur at higher values (~ 1.5 mJ, 2 J/cm^2) where a change in the ablation regime (Coulomb explosions) occurs, as indicated by the increasing in the $^{12}C^+$ signal. The mass spectra undergo important qualitative changes when extraction width pulse was varied. At short extraction widths (400 ns), it exist a cut-off for high masses, and the mass spectrum reveals atomic-only information. For longer width pulses (> 800 ns), higher mass fragments are detected, while low mass ion peaks reduce their intensity and resolution. These results allow a sort of modulation based on a simple modification in the extraction settings, not in the excitation conditions, opening the possibility of acquiring quasi-simultaneous atomic/molecular modulated mass spectra.

Two different procedures have been checked to detect surface traces of TNT that could be potentially valid for forensic analysis. Their usefulness to alert about possible presence of a nitroaromatic compound has been demonstrated, although additional work in determining the role played by the supporting substrate on the resultant spectra is still required.

ACKNOWLEDGMENTS

This work has been performed using funds from the Ministerio de Economía y Competitividad (Project CTQ2008-02197 and CTQ2011-24433) and from Consejería de Innovación, Ciencia y Empresa de la Junta de Andalucía (Project P07-FQM-03308). One of the authors (J.F.A.) would like to acknowledge the concession of a research grant from the Programa de Formaciónde Personal Investigador.

REFERENCES

[1] G.F. Adams, R.W. Shaw. Chemical reactions in energetic materials, *Annu. Rev. Phys. Chem.* 1992, 43, 311.

[2] C. Mullen, M. J. Coggiola, and H. Oser. Femtosecond laser photoionization time of flight mass spectrometry of nitro-aromatic explosives and explosives related compounds, *J. Am. Soc. Mass Spectrom.* 2009, 20, 419.

[3] D.F. McMillen, D.C. Erlich, C. He, C.H. Becker, D.A. Shockey. Fracture-induced and Thermal Decomposition of NTO Using Laser Ionization Mass Spectrometry, *Combust. Flame.* 1997, 111, 133.

[4] C. Kosmidis, K.W.D. Ledingham, A. Clark, A. Marshall, R. Jennings, J. Sander, R.P. Singhal. On the dissociation pathways of nitrobenzene, *Int. J. Mass Spectrom. Ion Processes.* 1994, 135, 229.

[5] M. Marshall and J.C. Oxley (Eds.), Aspects of explosives detection, Elsevier, Amsterdam, 2009

[6] J. Yinon (Ed.), Counterterrorist detection techniques of explosives, Elsevier, Amsterdam, 2007

[7] C.C. Garcia, J.M. Vadillo, J. Ruiz and J.J. Laserna. Nanometric in-depth characterization of P diffusion and TiO2 anti-reflective coatings in solar cells by laser ionization time of flight mass spectrometry, *J. Anal. At. Spectrom.* 2003, 18, 779.

[8] R. Huang, Q. Yu, L. Li, Y. Lin, W. Hang, J. He, B. Huang. High irradiance laser ionization orthogonal time of flight mass spectrometry: A versatile tool for solid analysis. *Mass Spectrom Rev.* 2011, 30, 1256.

[9] J.F. Alcántara, J.M. Vadillo J.J. Laserna. Two-pulse delayed 532-nm laser ionization of metals using collinear sub-threshold beams, *Rapid Comm. Mass Spectrom.* 2009, 22, 1999.

[10] J.F. Alcántara, J.M. Vadillo, J.J. Laserna. Subthreshold two-pulse time-delayed laser ionization of Cu, *Appl. Phys. A.* 2008, 92, 963.

[11] C. Mullen, A. Irwin, B. V. Pond, D. L. Huestis, M. J. Coggiola, H. Oser. Detection of explosives and explosives-related compounds by single photon laser ionization time-of-flight mass spectrometry, *Anal. Chem.* 2006, 78, 3807.

[12] J.F. Alcántara, J.M. Vadillo and J.J. Laserna. Experimental variables and matrix effects associated with the onset of ion generation in laser ionization of solid samples, *J. Anal. At. Spectrom.* 2010, 25, 1424.

[13] J.M. Vadillo, J.M.F. Romero, C. Rodriguez, J.J. Laserna. Effect of plasma shielding on laser ablation rate of pure metals at reduced pressure, *Surf. Int. Anal.* 1999, 27, 1009.

[14] H. Tellez, J.M. Vadillo, José J. Laserna. Secondary ion mass spectrometry of powdered explosive compounds for forensic evidence analysis. *Rapid Commun. Mass Spectrom.* 2012, 26, 1203.

[15] V.C. Jyothi Bhasu,M. Munawar Chadri M, J. Housden. Rapid mass spectrometric analysis of fragments of trinitrotoluene, picric acid and tetryl generated by laser irradiation. *J Mat Sci.* 1991, 26, 2199.

[16] S.M. Hankin, A.D. Tastker, L. Robson, K.W.D. Ledingham, X. Fang, P. McKenna, T. Mc Canny, R.P. Singhal, C. Kosmidis, P. Tzallas, D.A. Jaroszynski, D.R. Jones, R.C. Issac, S. Jamison. Femtosecond laser time of flight mass spectrometry of labile molecular analytes: laser-desorbed nitro-aromatic molecules. *Rapid Comm Mass Spectrom.* 2002, 16, 111.

[17] D.L. Huestis, C. Mullen, M.J. Coggiola, H. Oser. Laser-ionization mass spectrometry of explosives and chemical warfare simulants. *Int J High Speed Electron Systems.* 2008, 18, 159.

[18] K. Tönnies, R.P. Schmid, C. Weickhardt, J. Reif, J. Grotemeyer. Multiphoton ionization of nitrotoluenes by means of ultrashort laser pulses. *Int. J. Mass Spectrom.* 2001, 206, 245.

[19] B.V. Pond, C. Mullen, I. Suarez, J. Kessler, K. Briggs, S.E. Young, M.J. Coggiola, D.R. Crosley, H. Oser. Detection of explosive-related compounds by laser photoionization time-of-flight mass spectrometry. *Appl Phys A.* 2007, 86, 735

[20] F. Hillenkamp, J. Peter-Katalinic. MALDI MS: A Practical Guide to Instrumentation, Methods and Applications. Wiley, Amsterdam, 2007.

FIGURE CAPTIONS

Figure 1.	Schematic diagram of the experimental setup used for LIMS-TOF analysis
Figure 2.	Details of the ion extraction region
Figure 3.	Mass spectra (0-200 amu range) of 2,6-DNT obtained at different laser energies in the threshold range. The extraction pulse width was set to 800ns in these experiments. Each data set is represented at its maximum intensity, with an offset introduced to help in the comparison.
Figure 4.	Mass spectra (0-200 amu range) of 2,6-DNT obtained at laser energiesfrom 0.5mJ to 8mJ.The extraction pulse width was set to 800ns in these experiments. Each data set is represented at its maximum intensity, with an offset introduced to help in the comparison.
Figure 5.	Dependence of the ion signal with laser energy per pulse for $^{12}C^+$, $^{30}NO^+$, $^{63}C_5H_5^+$ and $^{148}(M\text{-}2OH)^+$ ion fragments.
Figure 6.	Mass spectra of 2,6-DNT at an energy per pulse of 1.3 mJ/pulse under different extraction widths conditions. The extraction delay was set at 0 ns.
Figure 7.	Comparative of the nanosecond TOF mass spectrum of laser desorption/ionization (top) and 70 eV electron impact NIST mass spectrum (down) of 2,6 DNT. Selected spectral features have been indicated.
Figure 8.	Single shot mass spectra of TNT traces sampled on Al conductive double side tape (a) and as a dried-drop of acetone-dissolved residue (b). Laser energy: 0.8 mJ/pulse; Wavelength: 266 nm.

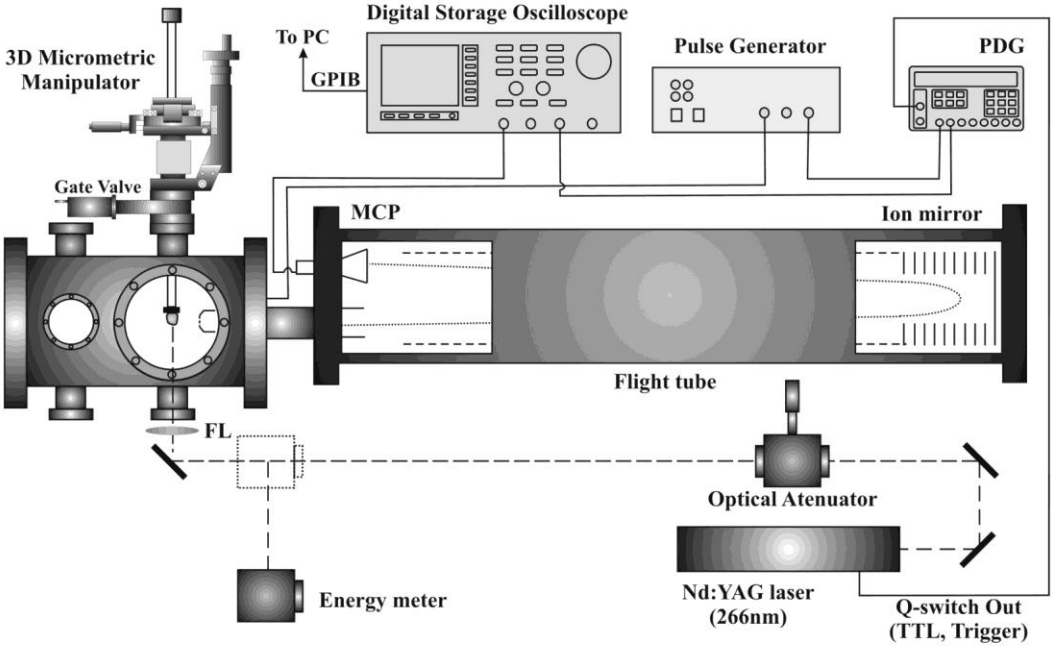
3D Micrometric Manipulator
To PC
GPIB
Digital Storage Oscilloscope
Pulse Generator
PDG
Gate Valve
MCP
Ion mirror
Flight tube
FL
Optical Atenuator
Energy meter
Nd:YAG laser (266nm)
Q-switch Out (TTL, Trigger)

Figure 1

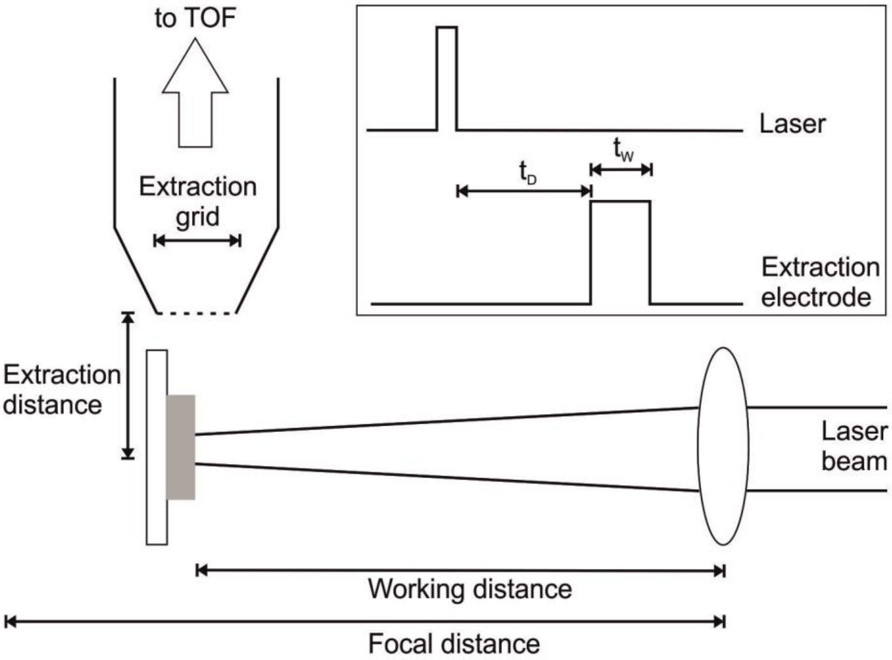
to TOF
Extraction grid
Laser
t_D
t_W
Extraction electrode
Extraction distance
Laser beam
Working distance
Focal distance

Figure 2

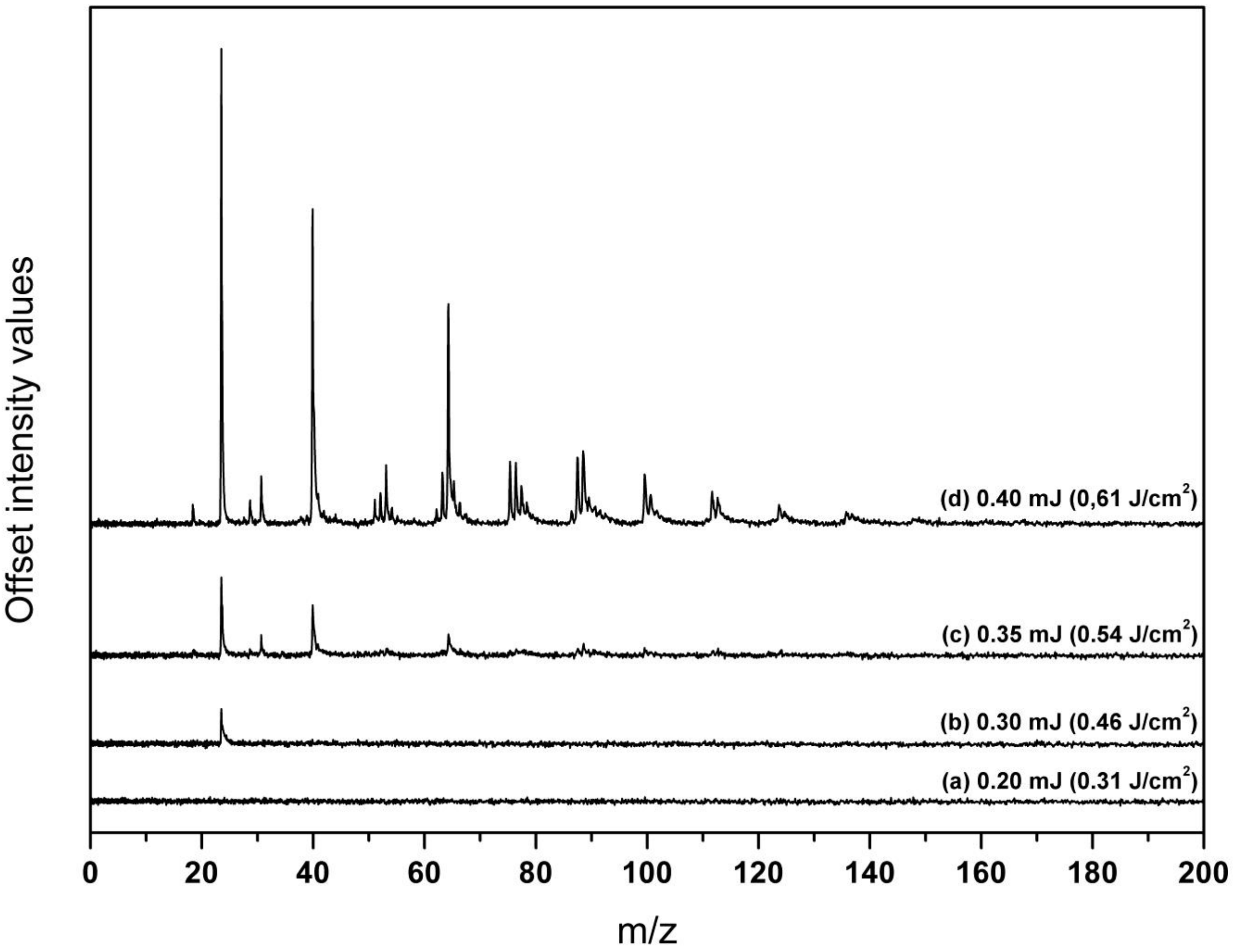
Offset intensity values
(d) 0.40 mJ (0,61 J/cm^2)
(c) 0.35 mJ (0.54 J/cm^2)
(b) 0.30 mJ (0.46 J/cm^2)
(a) 0.20 mJ (0.31 J/cm^2)
0
20
40
60
80
100
120
140
160
180
200
m/z

Figure 3

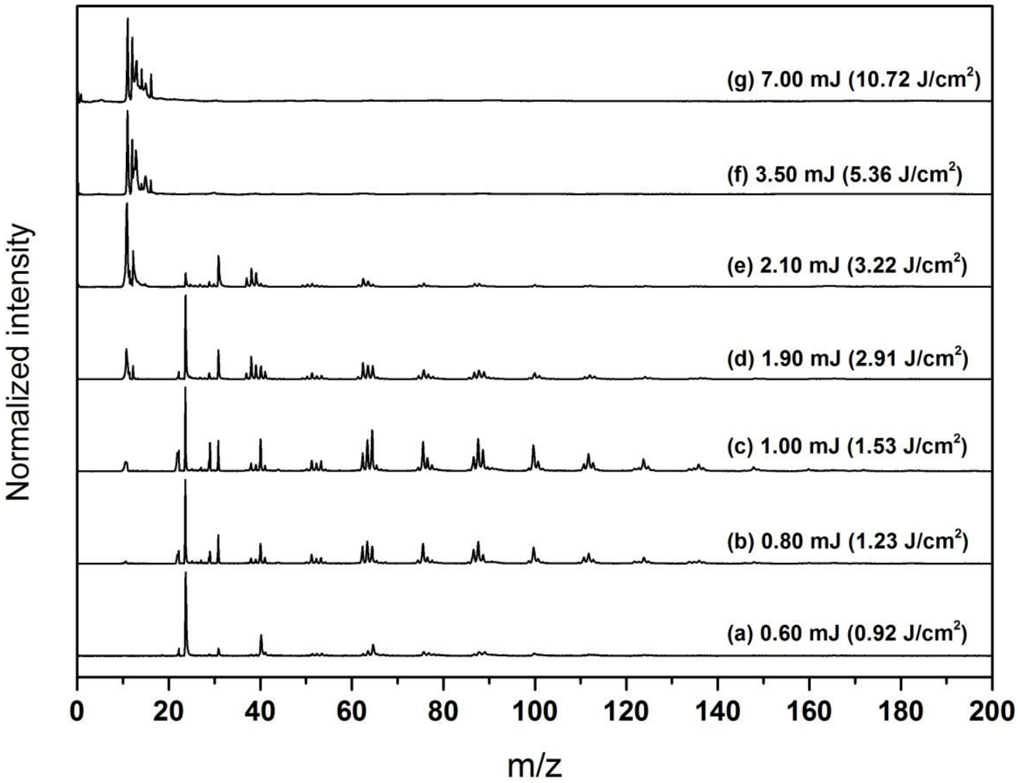
(g) 7.00 mJ (10.72 J/cm2)
(f) 3.50 mJ (5.36 J/cm2)
(e) 2.10 mJ (3.22 J/cm2)
(d) 1.90 mJ (2.91 J/cm2)
(c) 1.00 mJ (1.53 J/cm2)
(b) 0.80 mJ (1.23 J/cm2)
(a) 0.60 mJ (0.92 J/cm2)
Normalized intensity
0
20
40
60
80
100
120
140
160
180
200
m/z

Figure 4

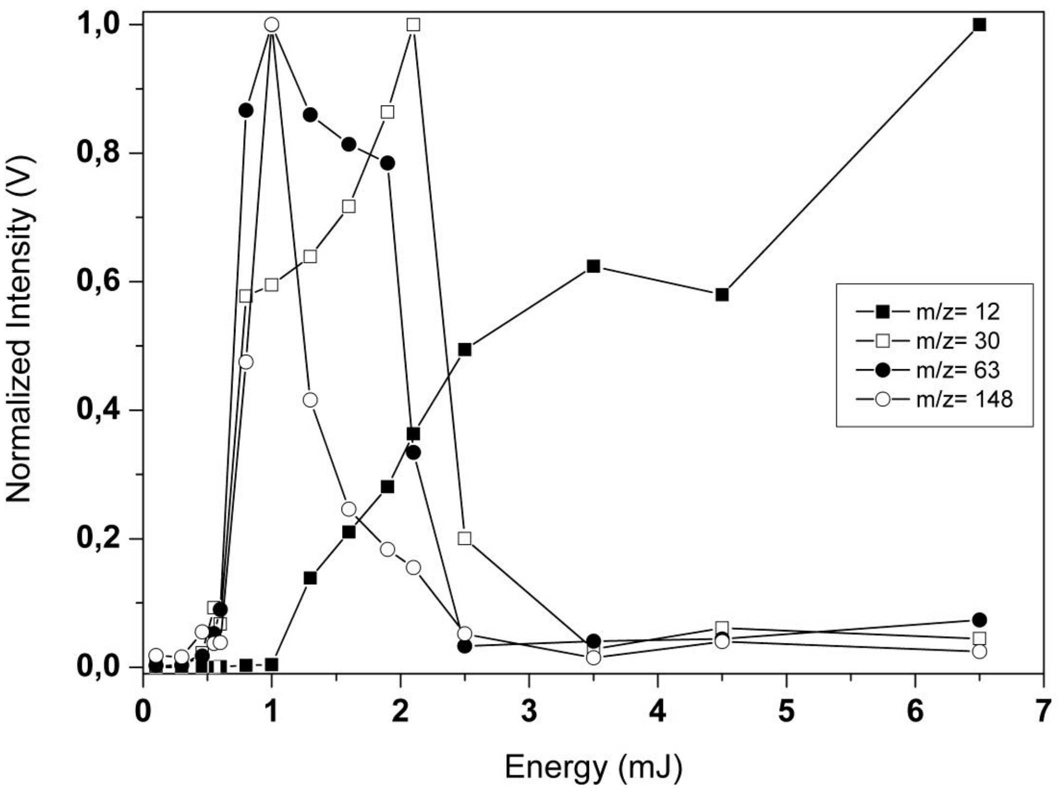
Normalized Intensity (V)
1,0
0,8
0,6
0,4
0,2
0,0
0
1
2
3
4
5
6
7
Energy (mJ)
m/z= 12
m/z= 30
m/z= 63
m/z= 148

Figure 5

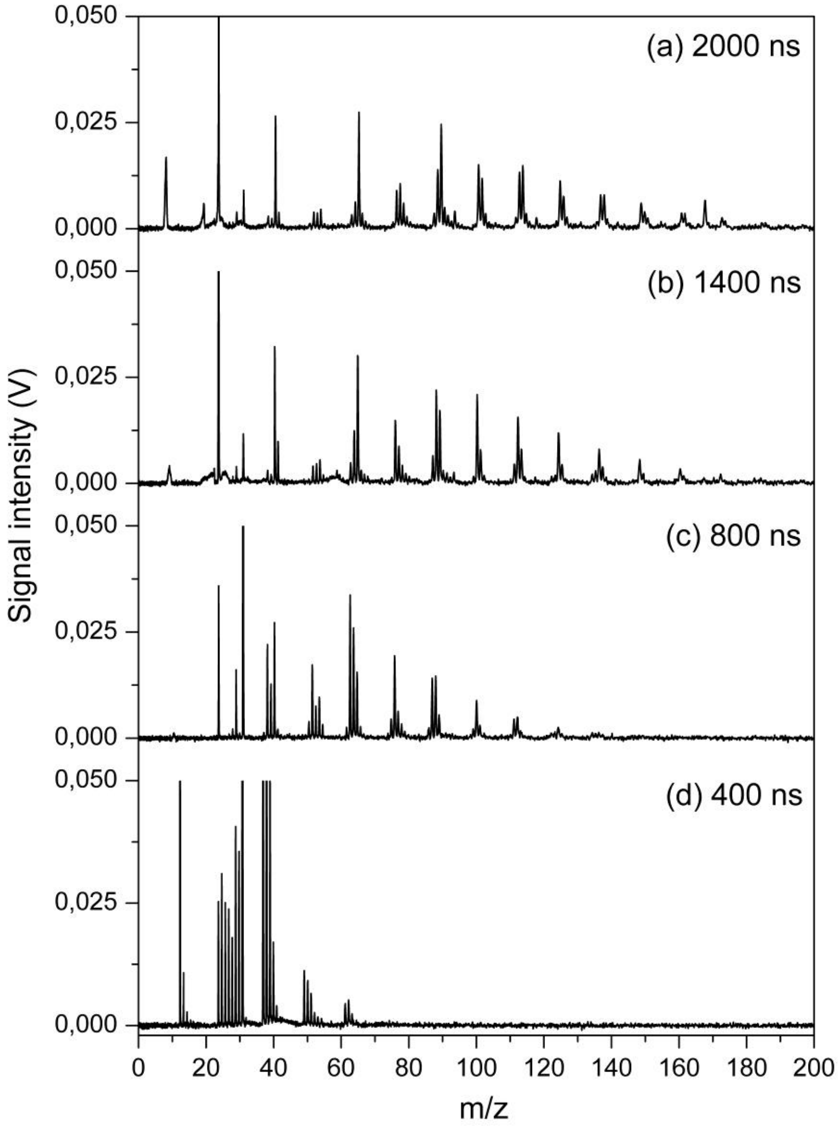
(a) 2000 ns
(b) 1400 ns
(c) 800 ns
(d) 400 ns
Signal intensity (V)
0,050
0,025
0,000
m/z
0
20
40
60
80
100
120
140
160
180
200

Figure 6

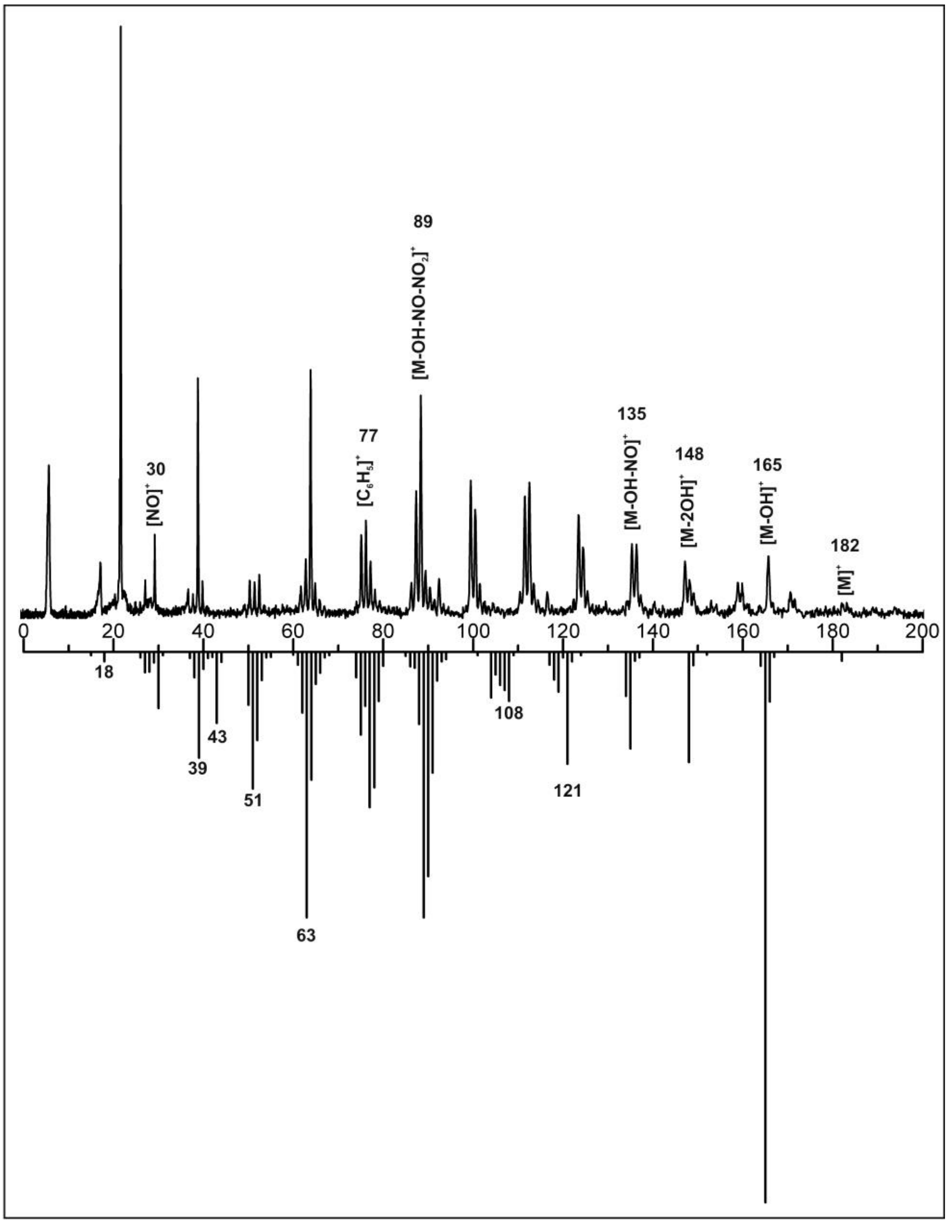
89
[M-OH-NO-NO$_2$]$^+$
77
[C$_6$H$_5$]$^+$
30
[NO]$^+$
135
[M-OH-NO]$^+$
148
[M-2OH]$^+$
165
[M-OH]$^+$
182
[M]$^+$
0
20
40
60
80
100
120
140
160
180
200
18
43
39
51
63
108
121

Figure 7

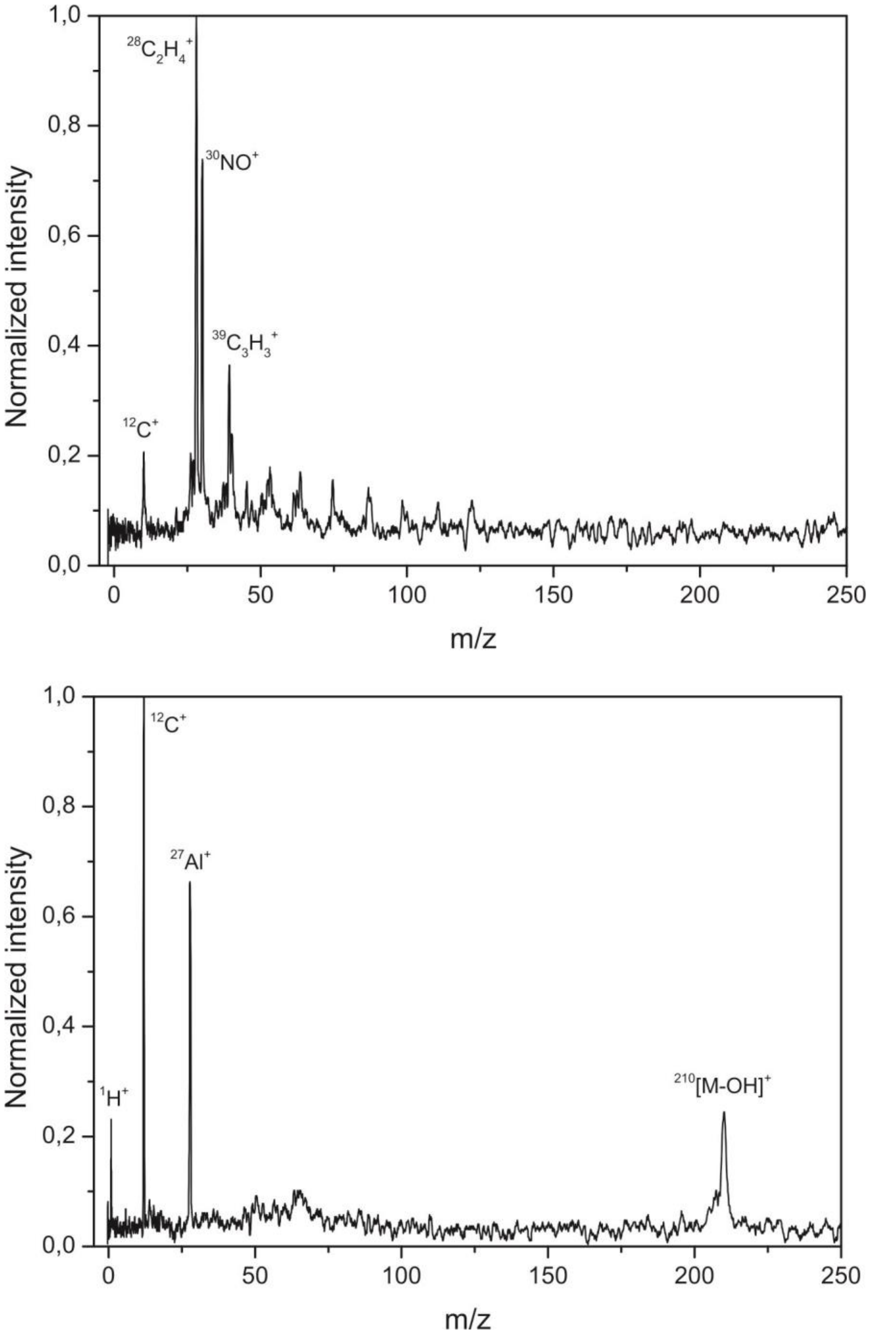
1,0
0,8
0,6
0,4
0,2
0,0
Normalized intensity
$^{28}C_2H_4^+$
$^{30}NO^+$
$^{39}C_3H_3^+$
$^{12}C^+$
0
50
100
150
200
250
m/z
1,0
0,8
0,6
0,4
0,2
0,0
Normalized intensity
$^{12}C^+$
$^{27}Al^+$
$^{1}H^+$
$^{210}[M\text{-}OH]^+$
0
50
100
150
200
250
m/z

Figure 8